 Related Commentary, page 3825

ApoE regulates hematopoietic stem cell proliferation, monocytosis, and monocyte accumulation in atherosclerotic lesions in mice

Andrew J. Murphy,[1] Mani Akhtari,[1] Sonia Tolani,[1] Tamara Pagler,[1] Nora Bijl,[1] Chao-Ling Kuo,[1] Mi Wang,[1] Marie Sanson,[2] Sandra Abramowicz,[1] Carrie Welch,[1] Andrea E. Bochem,[3] Jan Albert Kuivenhoven,[4] Laurent Yvan-Charvet,[1] and Alan R. Tall[1]

[1]Division of Molecular Medicine, Department of Medicine, Columbia University, New York, New York, USA. [2]Department of Medicine, Division of Cardiology, New York University School of Medicine, New York, New York, USA. [3]Department of Vascular Medicine and [4]Department of Experimental Vascular Medicine, Academic Medical Center, Amsterdam, The Netherlands.

Leukocytosis is associated with increased cardiovascular disease risk in humans and develops in hypercholesterolemic atherosclerotic animal models. Leukocytosis is associated with the proliferation of hematopoietic stem and multipotential progenitor cells (HSPCs) in mice with deficiencies of the cholesterol efflux–promoting ABC transporters ABCA1 and ABCG1 in BM cells. Here, we have determined the role of endogenous apolipoprotein-mediated cholesterol efflux pathways in these processes. In *Apoe*$^{-/-}$ mice fed a chow or Western-type diet, monocytosis and neutrophilia developed in association with the proliferation and expansion of HSPCs in the BM. In contrast, *Apoa1*$^{-/-}$ mice showed no monocytosis compared with controls. ApoE was found on the surface of HSPCs, in a proteoglycan-bound pool, where it acted in an ABCA1- and ABCG1-dependent fashion to decrease cell proliferation. Accordingly, competitive BM transplantation experiments showed that ApoE acted cell autonomously to control HSPC proliferation, monocytosis, neutrophilia, and monocyte accumulation in atherosclerotic lesions. Infusion of reconstituted HDL and LXR activator treatment each reduced HSPC proliferation and monocytosis in *Apoe*$^{-/-}$ mice. These studies suggest a specific role for proteoglycan-bound ApoE at the surface of HSPCs to promote cholesterol efflux via ABCA1/ABCG1 and decrease cell proliferation, monocytosis, and atherosclerosis. Although endogenous apoA-I was ineffective, pharmacologic approaches to increasing cholesterol efflux suppressed stem cell proliferative responses.

Introduction

Atherosclerosis is initiated by deposition of cholesterol-rich lipoproteins in the artery wall, leading to monocyte-macrophage recruitment and chronic inflammation. Prospective studies have documented a robust, risk-adjusted association between leukocytosis and cardiovascular disease (CVD) (1). While atherosclerosis-associated inflammation might contribute to this relationship, there is also considerable evidence that leukocytosis directly enhances atherosclerosis and thrombosis (1). Numerous CVD risk factors — including obesity, smoking, sedentary lifestyles and metabolic syndrome (including individual components of metabolic syndrome, such as high triglycerides and low HDL) — are all associated with leukocytosis (2–4). While these associations have usually been made for total wbcs or neutrophils, monocytosis has also been specifically associated with CVD and with atherosclerotic plaque burden in both prospective and cross-sectional studies (5–8). Monocytosis has also been linked to atherosclerosis in animal models: Gerrity first noted the relationship among dietary hypercholesterolemia, monocytosis, and atherosclerosis in swine and rabbit models (9, 10) and described an increase in BM colony forming units in hypercholesterolemic pigs (10). In the *Apoe*$^{-/-}$ mouse model of atherosclerosis, dietary hypercholesterolemia is associated with progressive monocytosis and an increase in the Ly-6C^{hi} (CCR2^{+}) subset of monocytes, which enter lesions more readily than do Ly-6C^{lo} monocytes (11, 12). Emerging evidence also suggests that neutrophilia can promote early lesion development (13, 14). Monocytosis in *Apoe*$^{-/-}$ mice has previously been shown to involve both increased production and decreased clearance of cells (11), but the detailed mechanisms underlying monocytosis and neutrophilia are poorly understood.

The ATP-binding cassette transporters ABCA1 and ABCG1 play an important role in mediating cellular cholesterol efflux to apoA-I and HDL, respectively (15). The absence of ABCG1 and ABCA1 in BM-derived cells in combination with hypercholesterolemia results in markedly accelerated atherosclerosis (16). These mice display dramatic expansion of myeloid cells, monocytosis, and neutrophilia, with an underlying proliferative defect of hematopoietic stem and multipotential progenitor cells (HSPCs) (17). HSPC hyperproliferation was linked to increased plasma membrane lipid rafts and increased plasma membrane levels of the common β subunit of the IL-3/GM-CSF receptor (CBS; also referred to as IL-3Rβ or CD131). Reversing the defect in cholesterol efflux via marked overexpression of transgenic *Apoa1* resulted in reduced expression of the CBS on HSPCs and abolition of the myeloproliferative phenotype (17). However, these studies did

Conflict of interest: Alan R. Tall serves on scientific advisory boards for Merck and Arisaph Pharmaceuticals and provides paid consulting services to Roche, Merck, Arisaph Pharmaceuticals, and CSL Limited related to the development of drugs that would increase HDL levels.

Citation for this article: *J Clin Invest.* 2011;121(10):4138–4149. doi:10.1172/JCI57559.

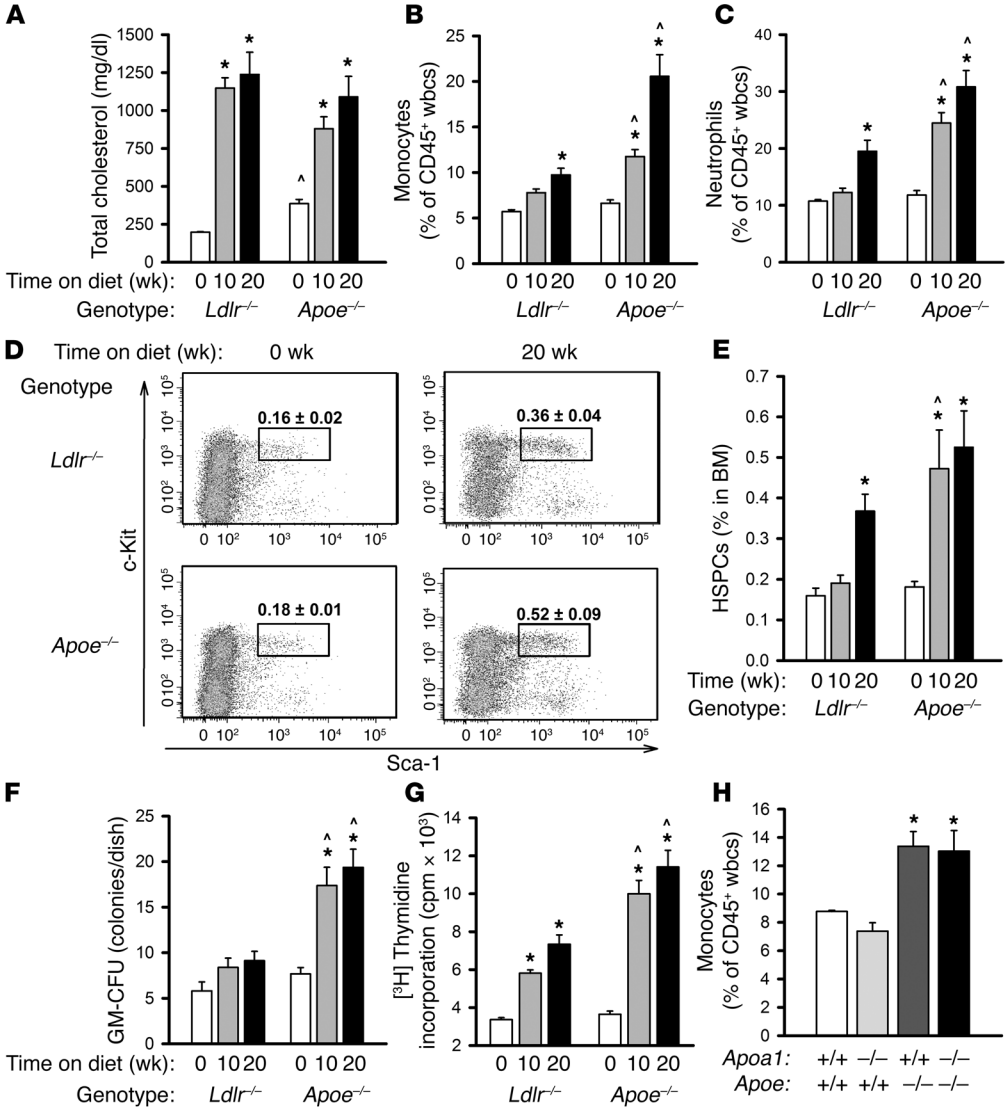

Figure 1

Feeding *Ldlr*$^{-/-}$ and *Apoe*$^{-/-}$ mice a WTD induces leukocytosis, expansion of HSPCs, increased GM-CFUs, and proliferation of BM myeloid cells. 8-week-old mice were fed a WTD for the indicated time periods. (**A**) Plasma cholesterol levels. (**B** and **C**) Monocytes and neutrophils were analyzed by flow cytometry and expressed as a percentage of CD45$^+$ leukocytes. (**D** and **E**) The HSPC population was assessed by flow cytometry and is expressed as a percentage of total BM cells. (**F**) GM-CFU assays from isolated BM. (**G**) BM proliferation was evaluated by [^{3}H]-thymidine incorporation into DNA. (**A**–**G**) **P* < 0.05 vs. 0 weeks; ^*P* < 0.05 vs. *Ldlr*$^{-/-}$ at the respective time point. Data are mean ± SEM, *n* = 6–8. (**H**) WT, *Apoa1*$^{-/-}$, *Apoe*$^{-/-}$, and *Apoa1*$^{-/-}$*Apoe*$^{-/-}$ mice were fed a chow diet until 20 weeks of age. The population of blood monocytes was identified by flow cytometry. **P* < 0.05 vs. WT. Data are mean ± SEM, *n* = 5–8.

not define the role of endogenous apolipoproteins in controlling HSPC proliferation. As noted above, ApoE has a prominent role in controlling leukocytosis, and ApoE and ApoE-containing HDL interact with ABCA1 and ABCG1, respectively, to promote cellular cholesterol efflux (16, 18, 19), but ApoE has not been linked to the control of HSPC proliferation. The goal of this study was to assess the role of endogenous apoA-I and ApoE in the control of HSPC proliferation and monocytosis.

Results

Hypercholesterolemia-associated leukocytosis is associated with expansion of HSPCs in Apoe$^{-/-}$ *mice.* Previous studies have documented neutrophilia and monocytosis in *Apoe*$^{-/-}$ mice, especially after feeding a high-fat, high-cholesterol Western-type diet (WTD) (11, 12). To determine whether this reflects HSPC proliferation, we analyzed blood and BM myeloid populations in *Apoe*$^{-/-}$ and *Ldlr*$^{-/-}$ mice in response to feeding a WTD for 10 or 20 weeks (Figure 1). *Apoe*$^{-/-}$ mice fed the WTD developed prominent monocytosis and neutrophilia (Figure 1, B and C; for absolute values, see Supplemental Figure 1, A and B; supplemental material available online with this article; doi:10.1172/JCI57559DS1). This was paralleled by a marked 3-fold expansion of the HSPC population in the BM (Figure 1, D and E), as well as an increase in GM-CFUs (Figure 1F) and increased proliferation of BM myeloid cells (as measured by [^{3}H]-thymidine incorporation into DNA; Figure 1G).

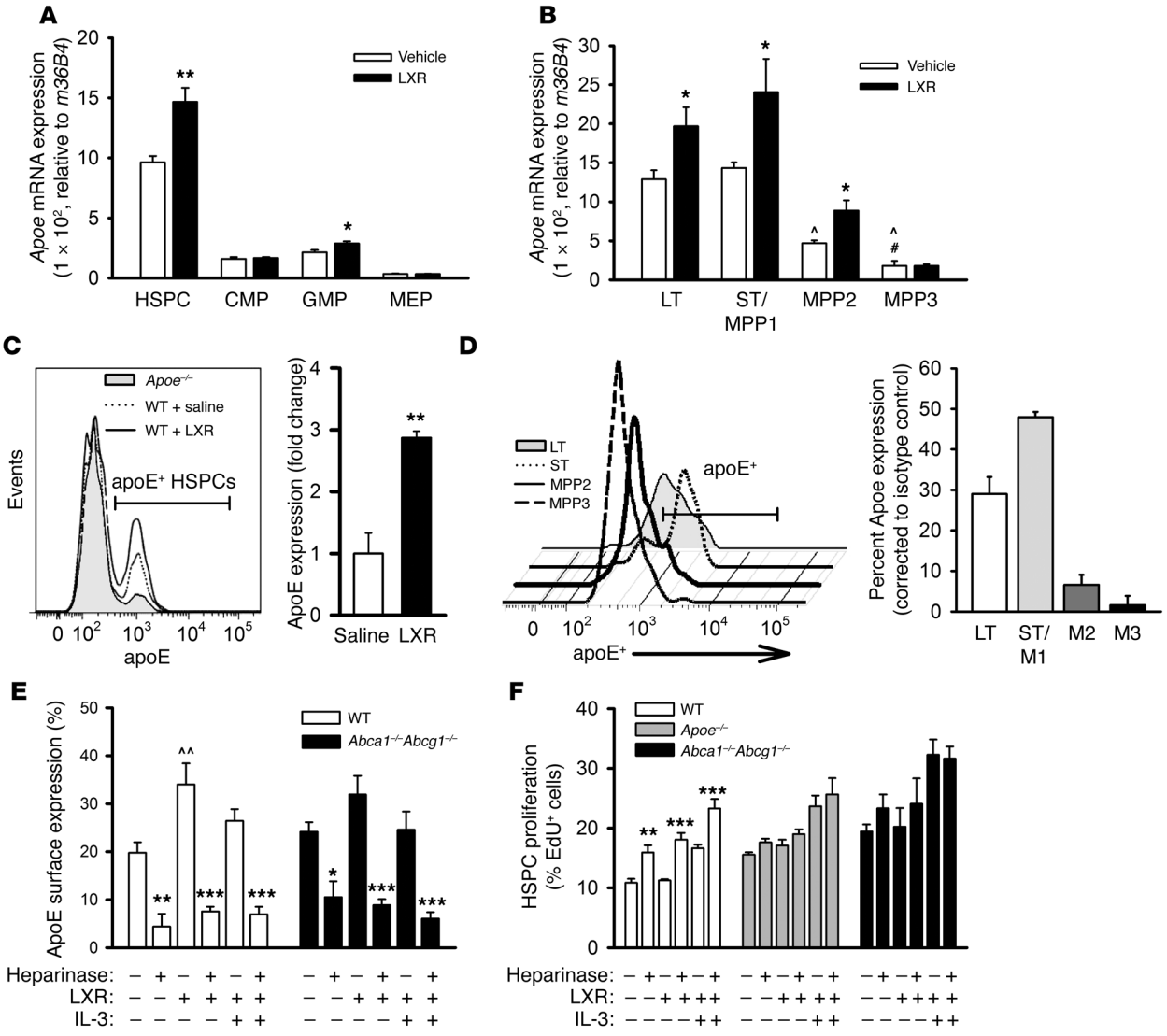

Figure 2

Apoe is expressed on the surface of HSPCs and interacts with *ABCA1* and *ABCG1* to modulate HSPC proliferation. (**A**–**D**) WT mice were injected with saline or LXR activator (T0901317, 25 mg/kg body weight). (**A** and **B**) HSPC and progenitor populations were isolated from the BM, cDNA was prepared, and different mRNAs were quantified by real-time PCR. Data are mean ± SEM (n = 5). (**A**) Expression in stem and progenitor cell subsets. *P < 0.05 vs. vehicle. (**B**) BM was subjected to FACS to obtain LT-HSC (LT), ST-HSC (ST) and MPP1, MPP2, and MPP3 subsets. *P < 0.05 vs. vehicle; ^P < 0.001 vs. LT; #P < 0.001 vs. ST. (**C** and **D**) ApoE protein was measured on the surface of (**C**) HSPCs and (**D**) HSPC subsets via flow cytometry. **P < 0.01 vs. vehicle. (**E** and **F**) BM was isolated, ApoE was cleaved from the surface using heparinase, and resynthesis of HSPGs was prevented using β-DX. BM cells were then incubated for 12 hours in IMDM with EdU (1 μM) with or without IL-3 and/or LXR activator (3 μM). (**E**) ApoE surface expression on HSPCs was measured via flow cytometry. (**F**) HSPC proliferation was determined by EdU incorporation. *P < 0.05, **P < 0.01, ***P < 0.001 vs. same treatment without heparinase; ^^P < 0.01 vs. no treatment. Data are mean ± SEM.

In contrast to the *Apoe*$^{-/-}$ mice, *Ldlr*$^{-/-}$ mice after 10 weeks on the WTD exhibited no significant monocytosis, slight neutrophilia (Supplemental Figure 1B), no expansion of HSPCs, and a 2-fold increase in BM myeloid proliferative response to exogenous growth factors (Figure 1G). After 20 weeks on the WTD, *Ldlr*$^{-/-}$ mice displayed modest increases in all of these parameters. There were significant genotype-specific effects for all blood and BM parameters (i.e., greater responses in *Apoe*$^{-/-}$ than in *Ldlr*$^{-/-}$ mice) at both 10 and 20 weeks (P < 0.05, ANOVA), even though blood cholesterol levels were higher in WTD-fed *Ldlr*$^{-/-}$ than *Apoe*$^{-/-}$ mice (Figure 1A). These findings suggest that increased proliferation and expansion of HSPCs may be at least partly responsible for the monocytosis and neutrophilia that develops in *Apoe*$^{-/-}$ and *Ldlr*$^{-/-}$ mice after feeding the WTD. The effects were much more prominent in *Apoe*$^{-/-}$ mice, suggestive of a specific role of ApoE in suppressing HSPC and BM myeloid proliferation.

Deficiency of Apoa1 in mice and in humans with Mendelian disorders causing low HDL is not associated with monocytosis. To directly compare the role of endogenous ApoE and apoA-I in control of HSPC proliferation and monocytosis, we assessed these phenotypes in chow-fed WT, *Apoa1*$^{-/-}$, *Apoe*$^{-/-}$, and *Apoe*$^{-/-}$*Apoa1*$^{-/-}$ mice. Whereas *Apoe*$^{-/-}$ mice showed significant monocytosis, there was no monocytosis in

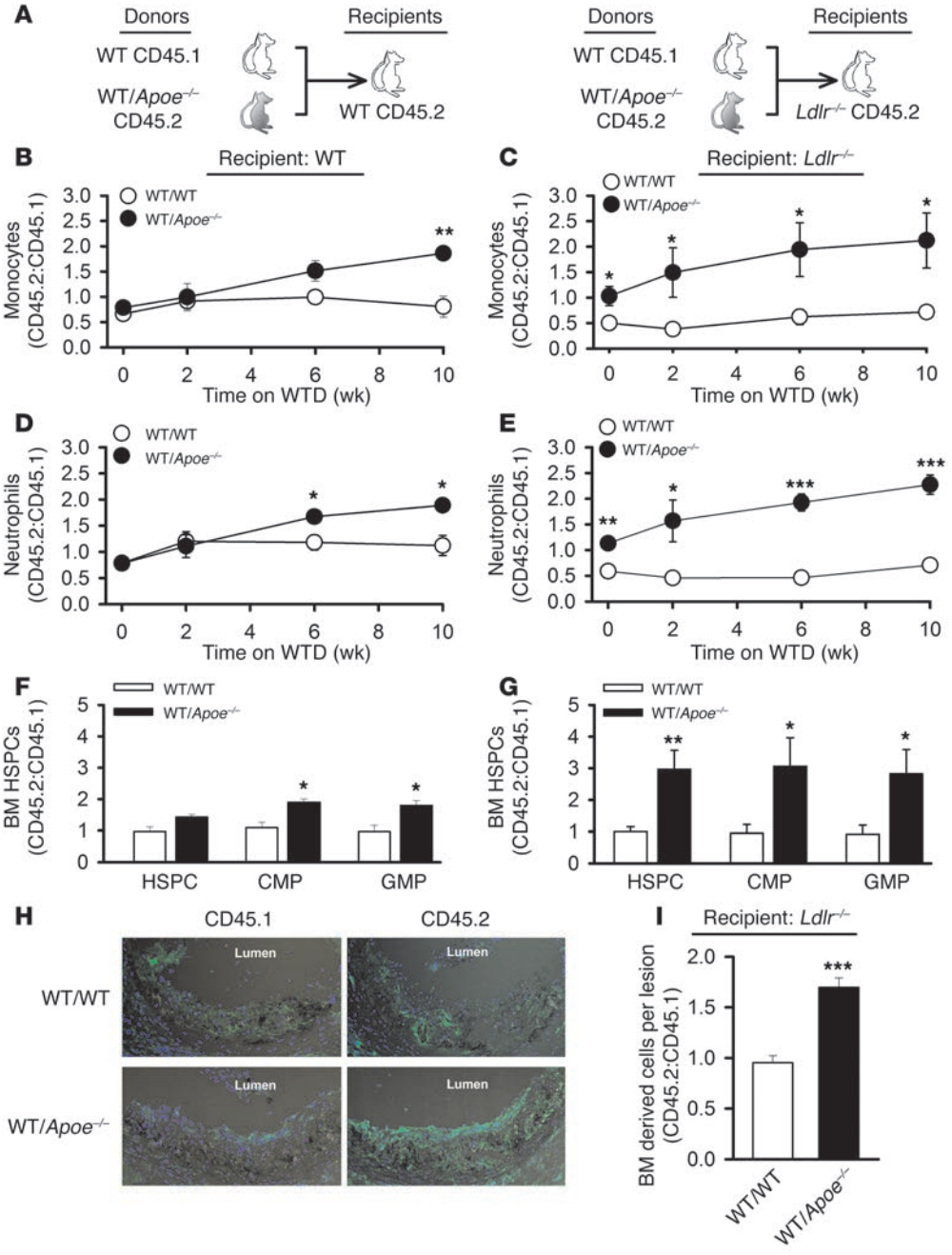

Figure 3

Leukocytosis and expansion of BM stem cells in *Apoe*$^{-/-}$ mice is cell autonomous and enhanced in a hypercholesterolemic environment, resulting in preferential accumulation of BM-derived cells in atherosclerotic lesions. (**A**) Experimental overview. Equally mixed portions of BM from the respective genotypes were transplanted into either WT or *Ldlr*$^{-/-}$ mice, which were fed a WTD for 10 weeks. (**B**–**G**) Ratio of CD45.2/CD45.1 monocytes over time (**B** and **C**), CD45.2/CD45.1 neutrophils over time (**D** and **E**), and CD45.2/CD45.1 BM stem cell populations (**F** and **G**) in WT (**B**, **D**, and **F**) and *Ldlr*$^{-/-}$ (**C**, **E**, and **G**) recipients. (**H** and **I**) Accumulation of CD45.1 or CD45.2 BM-derived cells in atherosclerotic lesions in *Ldlr*$^{-/-}$ recipients. (**H**) Representative stacked images of lesions from serial sections — stained for CD45.1 or CD45.2 (green); nuclei stained with TO-PRO-3 (blue) — presented as a combined overlay. Transmitted light images were all obtained by confocal microscopy (original magnification, ×20). (**I**) Accumulation of BM-derived cells (CD45.1- or CD45.2-positive cells per lesion) presented as a ratio of $CD45.2^+$ to $CD45.1^+$ cells in the lesion. Analysis was performed on 2 serial sections for either CD45.1 or CD45.2 cells for each mouse. $^*P < 0.05$, $^{**}P < 0.01$, $^{***}P < 0.001$ vs. WT/WT. Data are mean ± SEM ($n = 6$).

Apoa1$^{-/-}$ mice, and no additional monocytosis was observed when *Apoa1*$^{-/-}$*Apoe*$^{-/-}$ were compared with *Apoe*$^{-/-}$ mice (Figure 1H and Supplemental Figure 1C). There was also no expansion of HSPCs in *Apoa1*$^{-/-}$ compared with WT mice, and although *ApoA1*$^{-/-}$*Apoe*$^{-/-}$ mice did have expansion of their HSPCs compared with WT mice, this was not further increased compared with *Apoe*$^{-/-}$ mice (data not shown). Plasma cholesterol levels were lower in *Apoa1*$^{-/-}$*Apoe*$^{-/-}$ than in *Apoe*$^{-/-}$ mice (247 ± 14 mg/dl vs. 418 ± 38 mg/dl; mean ± SEM), consistent

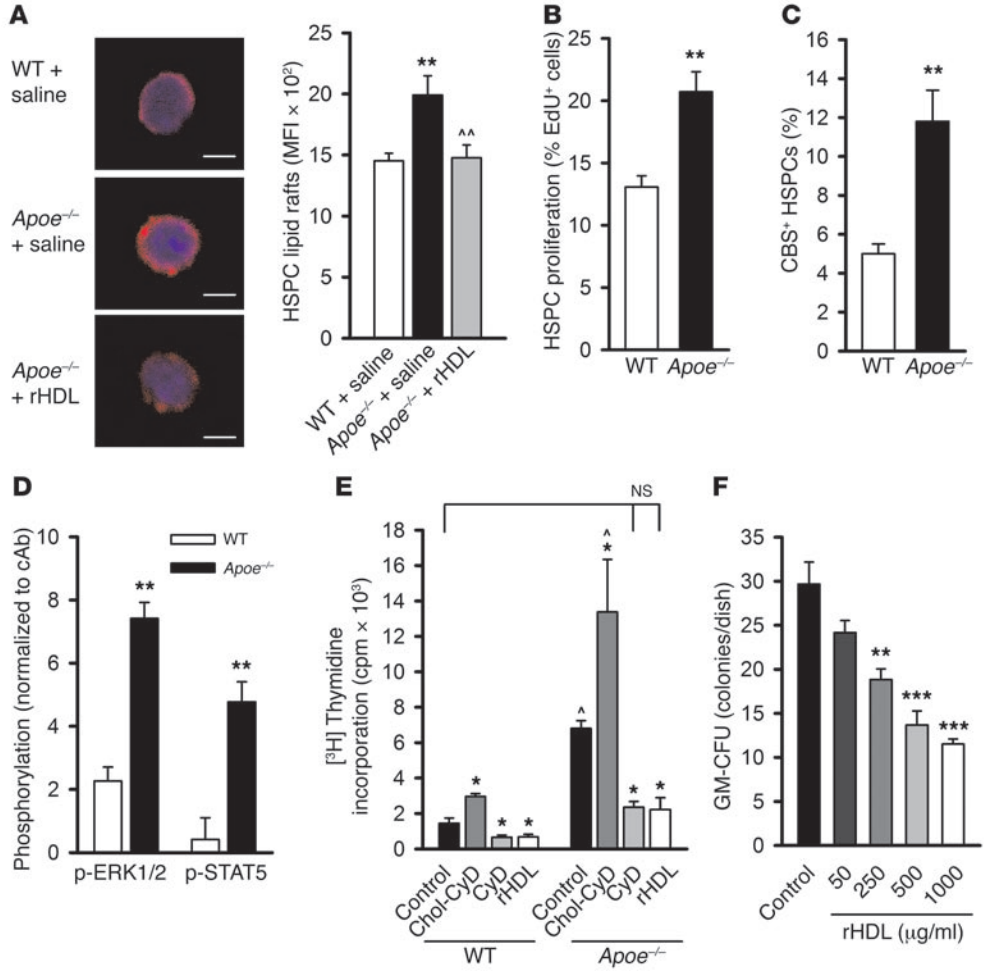

Figure 4

Cellular cholesterol levels modulate HSPC proliferation through the CBS. (**A**) WT and *Apoe*$^{-/-}$ mice were fed a WTD for 4 weeks and infused with saline or rHDL (80 mg/kg). 96 hours after infusion, HSPCS were isolated via flow cytometry and stained with CTx-B for lipid rafts. HSPCs were viewed on a confocal microscope, and lipid raft abundance was quantified. Scale bars: 5 μM. (**B**–**D**) WT and *Apoe*$^{-/-}$ mice were fed a WTD for 4 weeks, and BM HSPCs were analyzed by flow cytometry. (**B**) In vivo HSPC proliferation, determined by injecting mice with EdU 18 hours prior to sacrifice and assessing EdU incorporation into DNA. (**C**) Percent HSPCs expressing the CBS. (**D**) Phospho-flow for p-ERK1/2 and p-STAT5 in HSPCs. **P* < 0.05, ***P* < 0.01 vs. WT; ^^*P* < 0.01 vs. *Apoe*$^{-/-}$ plus saline. (**E**) BM was isolated from WT and *Apoe*$^{-/-}$ mice and incubated with IL-3 and GM-CSF in the presence or absence of cholesterol-loaded CyD (Chol-CyD; 6.6 mg/ml), CyD (6.6 mg/ml), or rHDL (1 mg/ml), and proliferation was assessed by [³H]-thymidine incorporation. **P* < 0.05 versus respective control; ^*P* < 0.05 vs. WT. (**F**) GM-CFU assay from BM isolated from *Apoe*$^{-/-}$ mice and incubated with increasing concentrations of rHDL. **P* < 0.05, ****P* < 0.001 vs. control. Data are mean ± SEM.

with previous reports (20), and this could have contributed to the lack of difference in monocytes between these groups. Nonetheless, these collective findings suggest that the role of endogenous ApoE is more important than that of apoA-I in controlling HSPC proliferation. We also determined whether there was significant monocytosis in humans with Mendelian disorders causing extremely low HDL cholesterol (HDL-C) and apoA-I levels. In a small study of humans with homozygous deficiencies of *Abca1* (Tangier disease) or lecithin-cholesterol acyltransferase (*Lcat*), there was no increase in blood monocyte or neutrophil counts (Supplemental Table 1).

A proteoglycan pool of ApoE on the surface of HSPCs controls cell proliferation. While *Apoe*$^{-/-}$ mice have elevated cholesterol and reduced HDL levels, our experiments pointed to a more specific role of ApoE in controlling HSPC proliferation. To determine whether ApoE is produced in HSPCs, we assessed in vivo mRNA levels in different populations of BM myeloid cells from WT mice with and without LXR activator treatment. *Apoe* showed highest expression in HSPCs relative to lineage committed progenitor populations, and was induced in HSPCs, and to a lesser extent in granulocyte-macrophage progenitors (GMPs), by LXR activator treatment (Figure 2A). In contrast, *Apoa1* mRNA was not detected in HSPCs. The HSPC population comprises long-term repopulating HSCs (LT-HSCs), short-term repopulating HSCs (ST-HSCs), and the multipotential progenitor (MPP) cell MPP1–MPP3 populations (21, 22). Analysis of different populations within the HSPC fraction showed that *Apoe* was most highly expressed in the stem cell–containing populations — in descending order, LT-HSCs and ST-HSCs/MPP1s, followed by MPP2s, and finally MPP3s — and was upregulated by LXR treatment in LT-HSC, ST-HSC/MPP1, and MPP2 subsets (Figure 2B). These findings are consistent with an earlier report based on microarrays, suggesting higher expression of *Apoe* mRNA in HSPCs relative to MPP cells (23). In contrast, *Abca1* and *Abcg1* were highly expressed and strongly induced by LXR activation in all HSPC subsets, with lower expression in myeloid progenitor populations (Supplemental Figure 2, A and B). Interestingly, flow cytometry revealed a pool of ApoE protein on the surface of WT HSPCs that was increased 2.8-fold after LXR activator treatment (Figure 2C). Cell surface ApoE was more prominent in the stem cell populations (i.e., LT-HSCs and ST-HSCs/MPP1s) than in MPP2s or MPP3s (Figure 2D). Combined treatment with heparinase to remove cell surface proteoglycans, and with 4-methylumbelliferyl β-D-xyloside (β-DX) to prevent their resynthesis (24), resulted in substantial loss of ApoE from the surface of HSPCs (Figure 2E), which suggests that ApoE was bound to proteoglycans on the surface of HSPCs.

To assess the hypothesis that the cell surface pool of ApoE acts to control proliferation of HSPCs, we measured proliferative responses after removal of heparan sulfate proteoglycans (HSPGs),

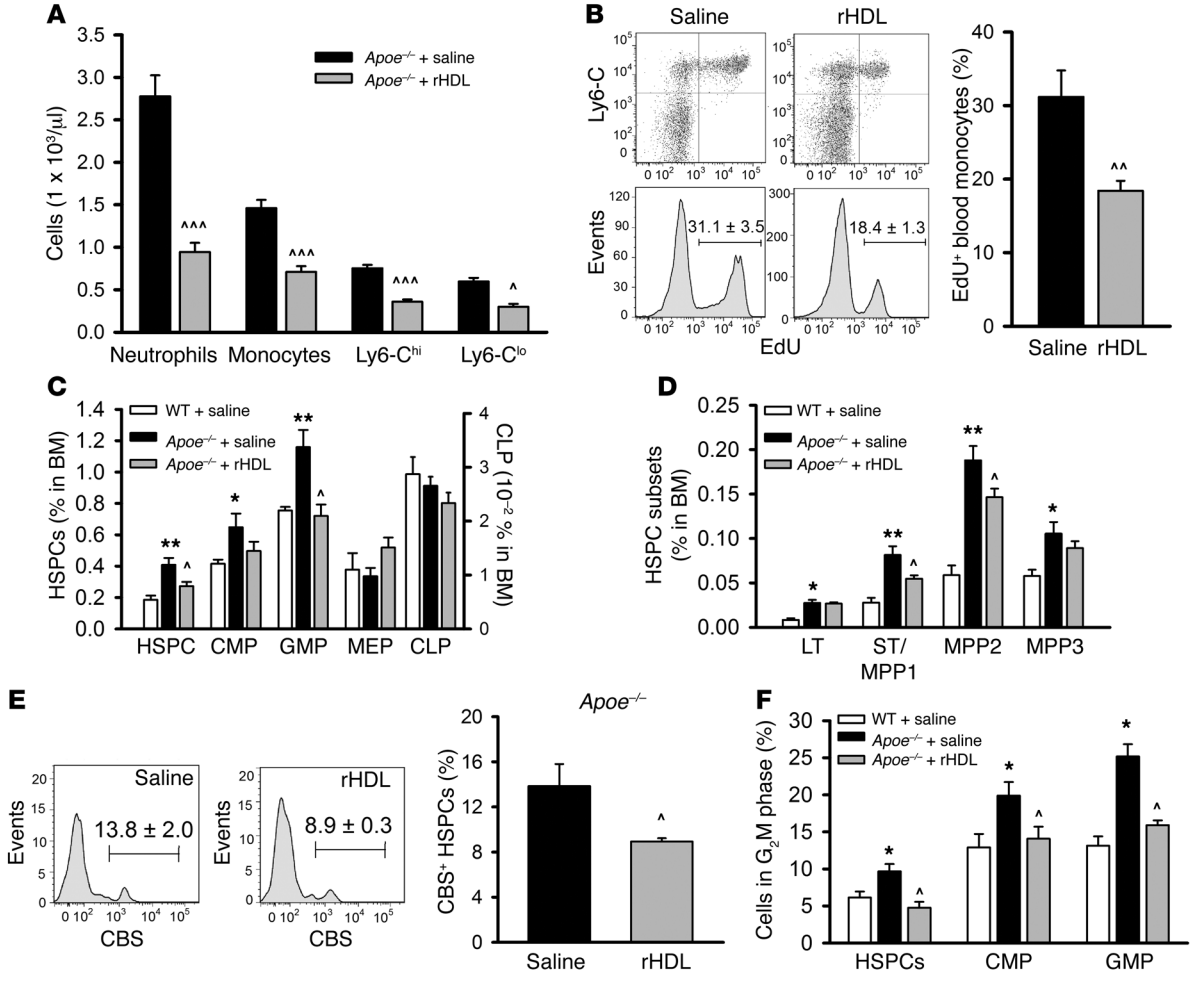

Figure 5

Infusion of rHDL attenuates monocytosis and neutrophilia by decreasing cellular cholesterol, CBS expression, and HSPC cell cycling in the BM of 4-week WTD-fed *Apoe*$^{-/-}$ mice. After WTD feeding for 4 weeks, *Apoe*$^{-/-}$ mice were infused with either saline or rHDL (CSL-111; 80 mg/kg), and analysis was performed after 7 days. (**A** and **B**) Blood experiments. Data are mean ± SEM (n = 8). (**A**) Monocytes were assessed via flow cytometry and converted to cells/μl using counts from the complete blood cell analyses. (**B**) Monocyte proliferation, determined by i.v. injection of EdU 18 hours prior to sacrifice. Proliferation was measured by EdU incorporation into blood monocytes, as determined by flow cytometry. (**C**–**F**) BM experiments. Data are mean ± SEM (n = 6–8). (**C**) HSPCs and downstream progenitors and (**D**) HSPC subsets, quantified by flow cytometry. (**E**) HSPCs expressing the CBS. (**F**) Percent cells in the G_2M phase of the cell cycle. (**A**–**F**) $^*P < 0.05$, $^{**}P < 0.01$, $^{***}P < 0.001$ vs. WT plus saline; $^{\wedge}P < 0.05$, $^{\wedge\wedge}P < 0.01$, $^{\wedge\wedge\wedge}P < 0.001$ vs. *Apoe*$^{-/-}$ plus saline.

including under conditions of LXR activation to increase cell surface ApoE and addition of exogenous growth factor (IL-3) to stimulate proliferation. Under all conditions, heparinase treatment led to significantly increased proliferation of WT, but not *Apoe*$^{-/-}$, HSPCs (Figure 2F). This indicates that proteoglycan-bound cell surface ApoE acts to suppress the proliferation of HSPCs. Heparinase treatment of *Abca1*$^{-/-}$*Abcg1*$^{-/-}$ HSPCs, albeit relatively effective at removing ApoE, did not increase their proliferation under any condition. Even though HSPC proliferation was greatest in *Abca1*$^{-/-}$*Abcg1*$^{-/-}$ compared with the other genotypes under basal conditions, this was still significantly increased in the presence of IL-3, which indicates that the cells' proliferative responses could still be modulated. This suggests that proteoglycan-bound ApoE requires expression of ABCA1 and ABCG1 to exert an antiproliferative effect, most likely by stimulating cholesterol and/or phospholipid efflux via the transporters.

ApoE acts in a cell-autonomous fashion to regulate myelopoiesis. The ability of ApoE to suppress HSPC proliferation in vivo could be mediated either by exogenous ApoE derived from the circulation or by ApoE made in HSPCs acting to control their own proliferation (Figure 2, E and F). To test the hypothesis that ApoE acts in vivo in an autocrine or cell-autonomous fashion, we performed competitive BM transplantation experiments. Equal portions of BM from WT CD45.1 and WT CD45.2 mice or from WT CD45.1 and *Apoe*$^{-/-}$ CD45.2 mice were transplanted into WT or *Ldlr*$^{-/-}$ recipients and, after BM reconstitution, were fed WTD for 10 weeks (Figure 3A). We chose *Ldlr*$^{-/-}$ rather than *Apoe*$^{-/-}$ recipients since introduction of WT BM into *Apoe*$^{-/-}$ mice results in marked lowering of plasma cholesterol levels (25, 26) that would act as a confounding variable affecting myeloid proliferation (i.e., mixture 1 would contain more WT BM and thus produce lower cholesterol levels than mixture 2). We confirmed that plasma cholesterol lev-

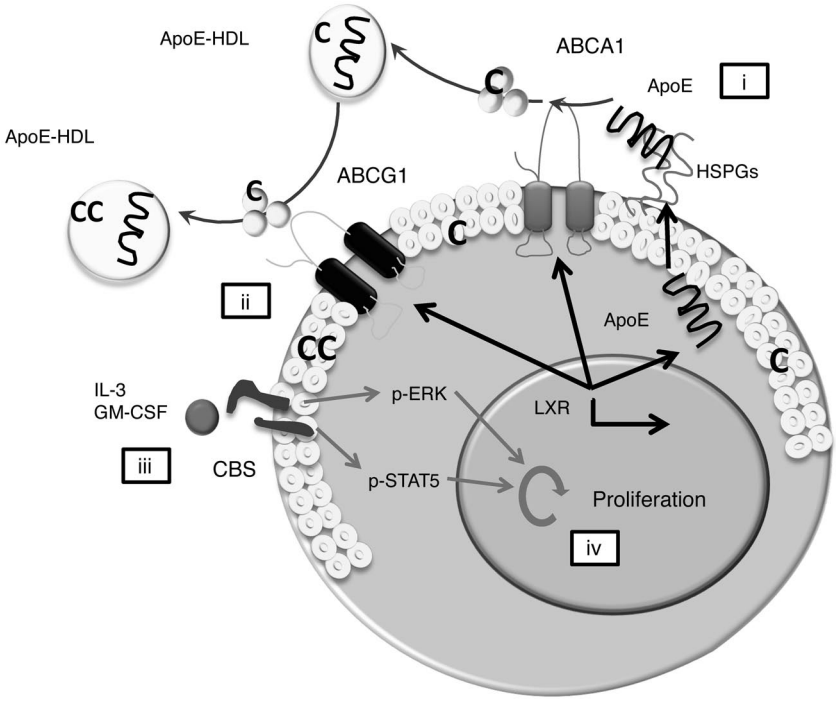

Figure 6
Endogenous cholesterol pathways regulate HSPC proliferation. HSPCs possess an active cholesterol efflux system expressing *Abca1*, *Abcg1*, and *Apoe*, which are responsive to LXRs. (i) ApoE protein is secreted and bound to cell surface HSPGs, inducing cholesterol efflux by interacting with ABCA1 and/or ABCG1. Importantly, circulating ApoE or ApoE from neighboring cells appears to be an inefficient acceptor of cholesterol (C) from HSPCs. (ii) In *Apoe*-deficient HSPCs, or when ApoE is removed from the cell surface by cleavage of the HSPGs, cholesterol efflux pathways are disrupted, and cholesterol begins to accumulate in the cells. (iii) This results in an increased population expressing the CBS, and the cells become hypersensitive to IL-3/GM-CSF signaling, inducing phosphorylation of EKR1/2 and STAT5. (iv) The net result is increased proliferation and expansion of HSPCs, leukocytosis, and accelerated atherosclerosis. Black and gray arrows denote antiproliferative and proliferative pathways, respectively.

els were indeed similar for recipients of WT+WT and WT+*Apoe*$^{-/-}$ BM (WT recipients, 138 ± 6 and 147 ± 4 mg/dl, respectively; *Ldlr*$^{-/-}$ recipients, 1,287 ± 97 and 1,552 ± 80 mg/dl, respectively; n = 6, mean ± SEM; P = NS for BM donor genotype effect). In WT recipients with very mild hypercholesterolemia, there was a greater contribution of *Apoe*$^{-/-}$ BM to blood monocytes and neutrophils, but only after prolonged WTD feeding (6–10 weeks; Figure 3, B and D). In hypercholesterolemic *Ldlr*$^{-/-}$ recipients, a competitive advantage of the *Apoe*$^{-/-}$ BM–derived blood monocytes and neutrophils was observed in moderately hypercholesterolemic conditions when mice were on a chow diet (i.e., 0 weeks), and this was markedly enhanced when the mice were fed WTD (Figure 3, C and E). Analysis of HSPCs and myeloid progenitors revealed increased numbers of *Apoe*$^{-/-}$ BM–derived (i.e., CD45.2) HSPCs, myeloid progenitors, monocytes, and neutrophils in both BM and spleen (Figure 3, F and G, and Supplemental Figure 4, A–F). Consistent with the findings on blood leukocytes, the cell-autonomous expansion of HSPCs, common myeloid progenitors (CMPs), and granulocyte-macrophage progenitors (GMPs) was much more prominent in hypercholesterolemic BM recipients than in chow-fed recipients. These findings revealed a cell-autonomous proliferative advantage of *Apoe*$^{-/-}$ HSPCs and myeloid progenitors in the BM and spleen, especially in a hypercholesterolemic environment, as an underlying cause of leukocytosis in hypercholesterolemic *Apoe*$^{-/-}$ mice.

Cell-autonomous expansion of Apoe$^{-/-}$ *HSPCs and leukocytosis results in increased leukocyte accumulation in atherosclerotic lesions*. Previous studies have shown that hypercholesterolemia-induced monocytosis in *Apoe*$^{-/-}$ mice is associated with increased monocyte entry into atherosclerotic plaques (11, 12). To determine whether the cell-autonomous expansion of monocytes also leads to increased accumulation of the *Apoe*$^{-/-}$ population of monocytes in plaques, we analyzed lesions from *Ldlr*$^{-/-}$ recipients. There was no preferential accumulation of WT CD45.1– versus WT CD45.2–specific BM–derived cells in the lesions of *Ldlr*$^{-/-}$ recipients (assessed as the percentage of nuclear stained cells that also stained for CD45.1 or CD45.2 in serial sections). However, there was a clear preponderance of *Apoe*$^{-/-}$ CD45.2–positive over WT CD45.1–positive cells (Figure 3, H and I), indicative of preferential accumulation of *Apoe*$^{-/-}$ BM–derived cells in plaques of *Ldlr*$^{-/-}$ mice that had been transplanted with mixed WT and *Apoe*$^{-/-}$ BM. Lesions showed positive staining with CD68, but not Ly6-G (data not shown), which indicated that accumulating cells were predominantly monocytes/macrophages, not neutrophils. As expected, the lesions in *Ldlr*$^{-/-}$ recipients transplanted with *Apoe*$^{-/-}$ CD45.2 BM were significantly larger than those in mice transplanted with WT CD45.2 BM (Supplemental Figure 5). These findings suggest that the increased cell-autonomous proliferation of *Apoe*$^{-/-}$ HSPCs led to monocytosis and increased entry of monocytes into lesions, contributing to the formation of larger lesions.

To determine a possible role of other mechanisms contributing to the preferential accumulation of *Apoe*$^{-/-}$ CD45.2 cells in lesions, we assessed some of the key steps of monocyte recruitment and entry into the lesion. This is a potentially important process in atherosclerotic lesion development, as ApoE appears to have little effect on the ability of macrophages to leave lesions (27). We found that *Apoe*$^{-/-}$ Ly6-C^{hi} monocytes had slightly increased expression of VLA-4 (17%), but not of other cell surface activation markers (Supplemental Figure 6, A–D). This was associated with an approximately 35% increase in *Apoe*$^{-/-}$ Ly6-C^{hi} monocyte adhesion to endothelial cells (Supplemental Figure 6, E and F). Ly6-C^{lo} monocytes were less adhesive than Ly6-C^{hi} cells, and there was no difference between the genotypes. Importantly, there was no difference in the migration of WT versus *Apoe*$^{-/-}$ Ly6-C^{hi} (CCR2^{+}) monocytes in response to MCP-1 (CCL2) in a Transwell migration assay (Supplemental Figure 6, G and H). These findings suggest that the increase in *Apoe*$^{-/-}$ CD45.2 cells in lesions may mainly reflect increased circulating monocyte numbers.

Increased membrane cholera toxin B staining, and higher levels of the CBS on the surface of Apoe$^{-/-}$ HSPCs, with enhanced signaling through ERK1/2 and STAT5. To determine whether deletion of *Apoe* in HSPCs causes reorganization of membrane lipids, we performed cholera toxin-B (CTx-B) staining. There was an increase in CTx-B staining of HSPCs from *Apoe*$^{-/-}$ mice (Figure 4A), consistent with an association between increased lipid raft formation and increased membrane cholesterol content (28–30). There also appeared to be an increase in neutral lipid in the HSPCs of *Apoe*$^{-/-}$ mice, as shown by increased staining with BODIPY 493/503 (Supplemental Figure 7 and refs. 31, 32). Increased incorporation of 5-ethynyl-2′deoxyuridine (EdU) into HSPCs (Figure 4B) indicated enhanced proliferation, consistent with data in Figure 1, and increased numbers of cells in the HSPC fraction expressed the CBS on their surface (Figure 4C). As the ligands for the CBS include IL-3 and GM-CSF, we next sought to determine whether related signaling pathways are activated in *Apoe*$^{-/-}$ HSPCs. Indeed, we observed an increase in p-ERK1/2 and p-STAT5 (Figure 4D), classical pathways involved in cell survival and proliferation (33–36). To link these findings with increased cholesterol content in the cell membrane (lipid rafts) and enhanced IL-3/GM-CSF signaling, we performed an in vitro proliferation assay, in which cholesterol levels in WT and *Apoe*$^{-/-}$ BM progenitor cells were modulated using cyclodextrin (CyD) (37, 38). *Apoe*$^{-/-}$ progenitors displayed increased proliferation compared with WT progenitors in response to IL-3/GM-CSF (Figure 4E). In both genotypes, increasing cellular cholesterol levels enhanced proliferation, and removal of cellular cholesterol by CyD or reconstituted HDL (rHDL; cholesterol-poor phospholipid/apoA-I complexes) decreased proliferation. Incubation of *Apoe*$^{-/-}$ BM cells with rHDL also showed a dose-dependent decrease in GM-CFUs (Figure 4F), indicative of a reduced capacity to produce leukocytes. These findings suggest that membrane cholesterol enrichment in *Apoe*$^{-/-}$ HSPCs leads to increased cell surface expression of the CBS and signaling via ERK and STAT5 pathways, leading to proliferation that can be reversed by cholesterol depletion using rHDL or CyD.

Infusion of rHDL suppresses leukocytosis and HSPC proliferation in Apoe$^{-/-}$ *mice.* To determine whether rHDL could reverse leukocytosis and HSPC proliferation in vivo, we gave a single infusion of rHDL (CSL-111) to 4-week WTD-fed *Apoe*$^{-/-}$ mice (39). Although there was a transient increase in HDL-C and apoA-I levels, total cholesterol (saline, 1,157 ± 143 mg/dl; rHDL, 1,080 ± 61 mg/dl; n = 10, P = NS) and HDL-C (saline, 33 ± 0.8 mg/dl, rHDL, 36 ± 3.2 mg/dl; n = 6, P = NS) remained unchanged 96 hours after infusion. There was a significant dose-related suppression of monocytosis and neutrophilia, with a nadir at about 1 week after infusion and a maximum effect at the 80-mg/kg rHDL dose, followed by a return to control levels after 14 days (Figure 5A and Supplemental Figure 8, A and B). A transient decrease in leukocytes seen at 24 hours was also observed in the saline group, likely representative of a nonspecific response. Both monocyte subsets, Ly6-C^{hi} and Ly6-C^{lo}, were suppressed (Figure 5A and Supplemental Figure 8, C and D). The reduction in blood monocyte numbers paralleled a decrease in EdU incorporation (Figure 5B), consistent with diminished proliferation of monocytes or their precursors.

To assess the effects of rHDL on BM HSPCs and myeloid populations, we sacrificed *Apoe*$^{-/-}$ or WT mice at 7 days after infusion of 80 mg/kg rHDL. This confirmed significant expansion of HSPC and myeloid precursor (CMP and GMP) populations, but not megakaryocyte-erythroid progenitor (MEP) or common lymphoid progenitor (CLP) populations, in *Apoe*$^{-/-}$ versus WT mice. There was a complete reversal of HSPC and myeloid progenitor expansion by rHDL infusion (Figure 5C). Analysis of HSPC subpopulations showed that LT-HSC, ST-HSC/MPP1, MPP2, and MPP3 populations were expanded in *Apoe*$^{-/-}$ mice, but only the ST/MPP1 and MPP2 populations were suppressed by rHDL (Figure 5D). Consistent with our proposed mechanism, rHDL infusion caused a reduction in lipid rafts and a decrease in the number of HSPCs expressing the CBS (Figure 5E). This led to a dampening of downstream signaling pathways (p-ERK1/2 and p-STAT5), which resulted in a decrease in HSPC proliferation, as determined by EdU incorporation (Supplemental Figure 9, A and B). Decreased proliferation was confirmed by a reduction in cell cycling of BM HSPCs, CMPs, and GMPs after rHDL infusion (Figure 5F). The spleen is a known reservoir for monocytes (40) and is home to a small population of HSPCs that actively produce leukocytes, especially under conditions of extramedullary hematopoiesis (41, 42). Therefore, we also examined the effect of rHDL infusion on splenic myeloid cells. There was a marked expansion of HSPCs, CMPs, and GMPs in the spleen of *Apoe*$^{-/-}$ mice, with increased EdU incorporation by CMPs and GMPs, but not HSPCs (Supplemental Figure 9, C and D). As in the BM, these changes were partly reversed by rHDL infusion.

Combined low-dose rHDL and LXR activator treatment reduces myeloid proliferation. We previously showed that LXR activators could suppress proliferation of BM myeloid cells in an ABCA1/ABCG1-dependent fashion (17). Since *Apoe*$^{-/-}$ mice have residual apoA-I–containing HDL, we reasoned that LXR activators would induce *Abca1*/*Abcg1* expression (Supplemental Figure 2), promote cholesterol efflux to endogenous or infused apoA-I–containing HDL, and suppress myeloid proliferation. Thus, we assessed the effects of LXR activator treatment and/or rHDL infusion on monocyte counts and HSPC proliferation in 4-week WTD-fed WT or *Apoe*$^{-/-}$ mice. We used a submaximal dose of 40 mg/kg, to bring out possible additive effects of LXR and rHDL treatments. The combined treatments significantly reduced monocyte and neutrophil counts, whereas single treatments did not have significant effects (Supplemental Figure 10, A and B). Unlike treatment with rHDL, LXR activator treatment did reduce monocyte counts in WT mice (Supplemental Figure 10, A and B), suggestive of an effect on additional pathways compared with rHDL. Single and combined treatments significantly decreased EdU incorporation into the monocytes in blood of *Apoe*$^{-/-}$ mice (Supplemental Figure 10C). Analysis of BM cells revealed that LXR activator or combined treatment significantly reduced the number and proliferation of HSPCs while suppressing expression of the CBS. These effects were only observed in WTD-fed *Apoe*$^{-/-}$ mice (Supplemental Figure 10, D–F). Together with data shown in Supplemental Figure 2, these findings suggest that in *Apoe*$^{-/-}$ mice, induction of *Abca1*/*Abcg1* in HSPCs by LXR activator treatments leads to cholesterol efflux to endogenous HDL or infused rHDL, leading to suppression of HSPC proliferation and reduced numbers of monocytes in blood.

Discussion

This study suggests a key role of cell surface proteoglycan-bound ApoE in controlling HSPC proliferation, myeloid cell expansion, monocytosis, and accumulation of monocytes in atherosclerotic lesions. ApoE appears to interact with ABCA1/ABCG1 in HSPCs, promoting cholesterol efflux and decreasing the cell surface expression and downstream signaling of the IL-3 receptor. Although

infusion of rHDL into *Apoe*$^{-/-}$ mice reversed these defects, circulating endogenous apoA-I and ApoE appeared to have relatively minor roles in controlling HSPC proliferation.

Even though ApoE is relatively abundant in the circulation, our studies revealed a major cell-autonomous role of ApoE in controlling proliferation of HSPCs and subsequent expansion of myeloid lineage cells. Apoe mRNA and cell surface protein were relatively abundant in the LT-HSC and ST-HSC populations, suggestive of a role in controlling stem cell proliferation and emergence from quiescence. Although *Abca1* and *Abcg1* were also highly expressed in HSPCs relative to other myeloid lineage cells, they were equally expressed in multipotential progenitor and stem cells, pointing to a key regulatory role of ApoE on stem cells. We documented an LXR-inducible pool of ApoE on the surface of HSPCs and showed that cell surface ApoE was bound to proteoglycans. Heparinase treatments indicated that proteoglycan-bound cell surface ApoE acts to suppress HSPC proliferation. In contrast, heparinase treatment did not affect proliferation of *Abca1*$^{-/-}$*Abcg1*$^{-/-}$ HSPCs, even though it resulted in release of ApoE from the surface of these cells. This genetic evidence is consistent with a model in which ApoE concentration at the cell surface by HSPGs facilitates its interaction with ABCA1/ABCG1, promoting cholesterol and/or phospholipid efflux (Figure 6). This conclusion is also supported by the similar downstream effects of ApoE and ABCA/ABCG1 deficiencies: cholesterol accumulation, increased cell surface levels, and signaling of the CBS via ERK and STAT5 signaling pathways (Figure 6). These findings are reminiscent of the binding of ApoE to the surface of hepatocytes or macrophages by interaction with HSPGs (24) and could explain the observation that ApoE expressed within macrophages is more effective at promoting cholesterol efflux than ApoE added to media (43).

The competitive BM transplantation experiments strongly suggest a causal link between the cell-autonomous effects of ApoE on the proliferation of HSPCs and myeloid cells and the number of leukocytes in atherosclerotic lesions (Figure 3). This is consistent with prior studies showing that monocytosis in WTD-fed *Apoe*$^{-/-}$ mice is associated with increased entry of monocytes into lesions (11, 12) and the strong genetic evidence indicating that the blood monocyte count is rate-limiting for the extent of atherosclerotic lesion development in both *Ldlr*$^{-/-}$ and *Apoe*$^{-/-}$ mice (44–47). There may be additional mechanisms involved in accumulation of *Apoe*$^{-/-}$ leukocytes, such as increased monocyte activation, endothelial transmigration, or retention. Examination of these processes showed that *Apoe*$^{-/-}$ Ly6-C^{hi} monocytes were slightly activated and had a moderate increase in adhesion to endothelial cells. However, *Apoe*$^{-/-}$ monocytes may be primed to respond to in situ activation signals, and this could also play a significant role in atherogenesis in vivo. We did not determine a potential effect of ApoE on monocyte or macrophage egress from lesions; however, a recent study indicates that ApoE does not likely affect this process (27). Given the magnitude of the 3- to 4-fold cell-autonomous increases in neutrophil and monocyte counts arising from *Apoe* deficiency (Figure 3, C and E), this is likely to be an important mechanism underlying monocyte accumulation in lesions in *Apoe*$^{-/-}$ mice.

Pioneering studies have shown that transplantation of WT BM into *Apoe*$^{-/-}$ mice leads to a marked decrease in atherosclerosis, associated with reductions in plasma cholesterol levels (48), which illustrates the central role of ApoE in the clearance of chylomicron and VLDL remnants (49). Our findings are consistent with earlier reports indicating that ApoE in BM-derived cells also exerts antiatherogenic effects independent of its ability to lower cholesterol levels or to alter the lipoprotein profile (26, 50). Although these effects were likely mediated in part through expression of ApoE in lesional macrophages, our present results suggest that effects on HSPC and myeloid cell proliferation may also have been involved.

Even though endogenous circulating apoA-I and HDL were relatively ineffective at controlling HSPC proliferation, infusion of pharmacological doses of cholesterol-poor phospholipid/apoA-I complexes (i.e., rHDL) could reverse these defects. Increasing HDL levels in *Apoe*$^{-/-}$ mice and other atherosclerosis models, either by infusions of HDL or transgenic overexpression of *Apoa1*, has consistently been shown to reduce atherosclerosis (51). In the present studies, we used a preparation of rHDL (CSL-111) previously shown to cause regression of coronary atherosclerosis, stabilization of peripheral vascular lesions, and decreased inflammation in humans at doses similar to those used here (80 mg/kg) (39, 52–54). rHDL suppressed HSPC and GMP proliferation in BM and spleen and reduced blood monocyte and neutrophil counts. Although we showed that the intrinsic cholesterol efflux pathway mediated by ApoE in HSPCs was more important than circulating HDL in controlling their proliferation, infusions of rHDL (cholesterol free particles with a high cholesterol efflux potential) also altered membrane lipid rafts of HSPCs, suppressing proliferation and monocytosis. This pharmacologic effect likely reflects the large dose of rHDL — the effect was seen at 80 but not 40 mg/kg (Supplemental Figure 8) — with a high cholesterol efflux capacity. Moreover, the acute infusion will result in rapid removal of cellular cholesterol, while the longstanding depletion of *Apoa1* in the knockout model may be compensated by changes in cholesterol homeostasis (such as increased synthesis) as well as other efflux pathways, notably ApoE. We also showed that LXR activation, alone or in combination with a low dose of rHDL, reduced HSPC proliferation and monocytosis. LXR activators induced *Abca1*, *Abcg1*, and *Apoe* in HSPCs, and LXR activators appeared to be acting via a mechanism similar to that of rHDL, i.e., by decreasing the cell surface expression of the CBS on HSPCs. However, LXRs are widely expressed with many target genes, and additional mechanisms may be involved.

In conclusion, we describe a mechanism that we believe to be novel, in which ApoE acts in a cell-intrinsic fashion to regulate HSPC proliferation, monocytosis, and neutrophilia, likely by promoting cholesterol efflux from HSPCs via ABCA1/ABCG1. Importantly, we have also shown that treatment with pharmacological doses of the potent cholesterol acceptor rHDL bypassed this cell-intrinsic mechanism and restored normal HSPC proliferative responses and blood leukocyte levels in the setting of atherosclerosis. This could represent a novel antiatherogenic mechanism of rHDL infusions.

Methods

Animals

WT (C57BL/6), *Apoe*$^{-/-}$ (B6.129P2-*Apoe*^{tm1Unc}), *Ldlr*$^{-/-}$ (B6.129S7-*Ldlr*^{tm1Her}), *Apoa1*$^{-/-}$ (B6.129P2-*Apoa1*^{tm1Unc}/J), and WT congenic CD45.1$^{+/+}$ (B6.SJL-Ptprca–Pep3b-/BoyJ) mice were purchased from The Jackson Laboratory. *Apoe*$^{-/-}$ and *Apoa1*$^{-/-}$ mice were crossed to obtain *Apoe*$^{-/-}$*Apoa1*$^{-/-}$ mice. *Abca1*$^{-/-}$*Abcg1*$^{-/-}$ mice were bred as previously described (16). At 8 weeks of age, mice were placed on a WTD (21% milk fat, 0.2% cholesterol; catalog no. TD88137; Harlan Teklad) for the specified amount of time. Treatments with rHDL (provided by CSL Australia) or vehicle (saline) was administered

via the tail vein. Mice were treated with the LXR agonist T0191317 (Cayman Chemical; 25 mg/kg body weight for 3 consecutive days in DMSO/saline) or vehicle (DMSO/saline) via intraperitoneal injections (55).

Human studies

Homozygotes or compound heterozygotes for LCAT mutations all presented with the clinical phenotype of fish eye disease (56–58). Tangier disease patients were previously described (59, 60) and have deleterious mutations on both alleles. Controls were healthy and matched for age and sex. Mutations for each of the patients are listed in Supplemental Table 2. Blood was obtained after an overnight fast in EDTA-coated tubes, and plasma was obtained and stored using standardized protocols. Plasma cholesterol, LDL cholesterol, and HDL-C were analyzed using commercially available kits (Randox). Plasma apoA-I was measured using a commercially available turbidometric assay (Randox). All analyses were performed using the Cobas Mira autoanalyzer (Roche). Routine complete blood cell analysis with differentials was preformed to obtain total wbcs, monocytes, and neutrophils.

Cholesterol acceptors/donators

rHDL. rHDL was provided by CSL Behring AG; CSL-111 is composed of human apoA-I and phosphatidylcholine from soybean in a 1:150 ratio. Injectable solutions of rHDL were prepared under sterile conditions.

Cyd and cholesterol-loaded CyD. CyD (methyl-β-cyclodextrin; Sigma-Aldrich) and cholesterol-loaded CyD were prepared as described previously (38, 61). Cellular cholesterol was depleted or loaded by 6.6 mg/ml CyD or cholesterol-loaded CyD for 30 minutes before growth factor treatment.

Mouse total cholesterol

Total cholesterol levels were measure from the plasma of mice using the Cholesterol E kit (Wako Diagnostics) per the manufacturer's instructions.

Mouse wbc counts

Total wbc counts were obtained from freshly drawn blood via tail bleeding and quantified using the FORCYTE Veterinary Analyzer (Oxford Science Inc.).

Flow cytometry

Blood leukocytes. For identification of monocytes and neutrophils from whole blood, we used the following strategy. Blood was drawn via tail bleeding and collected into EDTA-lined tubes, which were immediately incubated on ice. All subsequent steps were performed on ice. rbcs were lysed (BD pharm Lyse; BD Biosciences), and wbcs were centrifuged, washed, and resuspended in HBSS (0.1% BSA w/v, 5 mM EDTA). Cells were stained with a cocktail of antibodies against CD45-APC-Cy7, Ly6-C/G-PerCP-Cy5.5 (BD Biosciences — Pharmingen), CD115-APC, and CD11b-FITC (eBioscience). Samples were analyzed on an LSR-II (BD Biosciences). Monocytes were identified as $CD45^{hi}CD115^{hi}$ and further subdivided into Ly6-C^{hi} and Ly6-C^{lo}; neutrophils were identified as $CD45^{hi}CD115^{lo}$Ly6-C/G^{hi} (Gr-1). CD11b, CD11c, VLA-4 MFI and percent $CD62L^{+}$ was measured on Ly6-C^{hi} monocytes as a marker of activation (38, 62).

HSPCs. BM was harvested from the femurs and tibias and subjected to a brief rbc lysis. BM was resuspended in HBSS (BSA/EDTA) and incubated with a cocktail of antibodies to lineage committed cells (CD45R, CD19, CD11b, CD3e, TER-119, CD2, CD8, CD4, and Ly-6G; all FITC; eBioscience) and stem cell markers Sca1-Pacific Blue and ckit-APC Cy7. HSPCs were identified as $lin^{-}Sca1^{+}ckit^{+}$. Where further identification of hematopoietic progenitor cells was required, antibodies to CD16/CD32 (FcγRII/III) and CD34 were used to separate CMP ($lin^{-}Sca1^{-}ckit^{+}CD34^{int}$FcγRII/$III^{int}$), GMP ($lin^{-}Sca1^{-}ckit^{+}CD34^{int}$FcγRII/$III^{hi}$), and MEP ($lin^{-}Sca1^{-}ckit^{+}CD34^{lo}$FcγRII/$III^{lo}$). To further separate HSPC subsets, antibodies to CD135 (flt3), CD150 (Slamf1), and CD34 were used, and subsets were identified as LT-HSC ($CD150^{hi}CD34^{lo}$), ST-HSC and MPP1 ($CD150^{hi}CD34^{int}$), MPP2 ($CD150^{lo}CD34^{int}CD135^{lo}$), and MPP3 ($CD150^{lo}CD34^{int}CD135^{hi}$). ApoE was measured on the cell surface of HSPCs using a primary antibody to ApoE (Biodesign) followed by incubation with a PE-conjugated secondary antibody (Abcam); $Apoe^{-/-}$ and isotype controls showed a similar low nonspecific signal in these assays (Figure 2C and Supplemental Figure 3). Phospho-flow was performed using antibodies to either p-ERK1/2 or p-STAT5 (BD Biosciences). Neutral lipid was measured using BODPIY 493/503 (Invitrogen). Cells were run on either LSRII for analysis or FACSAria for sorting, both running FACSDiVa software.

GM-CFU assay

BM was isolated from WT, $Ldlr^{-/-}$, and $Apoe^{-/-}$ mice after WTD feeding for 0, 10, and 20 weeks. BM cells (4×10^4) were plated in methylcellulose-based media supplemented with an assortment of recombinant cytokines, including SCF, IL-3, and IL-6 (Methocult GF M3534; StemCell Technologies) supplemented with 2% FCS (StemCell Technologies). The number of GM-CFUs per dish was counted after 12 days of culture.

Thymidine proliferation assay

BM cells were isolated from the mice and, after a brief lysis and washing, were cultured in IMDM (Gibco; Invitrogen) containing 10% FCS for 2 hours to remove adherent (mature) cells enriching for progenitor cells. The nonadherent cells were then cultured for 72 hours in the presence of 100 ng/ml stem cell factor (CSF, ckit-ligand; R&D Systems), 6 ng/ml IL-3 (R&D Systems), and 2 ng/ml GM-CSF (R&D Systems). Cells were pulsed for the final 2 hours with 2 μCi/ml [^{3}H]-thymidine, and the radioactivity incorporated into the cells was determined by standard procedures using a liquid scintillation counter.

Real-time PCR analysis of HSPCs

HSPCs were isolated via fluorescent-activated cell sorting (FACS) directly into RLT lysis buffer. RNA was extracted using a RNeasy Micro Kit (Qiagen), and cDNA was synthesized using SuperScript VILO (Invitrogen). Initial differences in mRNA levels was controlled using the reference gene *m36B4*.

ApoE surface removal and proliferation studies

BM cells were isolated and subjected to a brief rbc lysis. Cells were then cultured for 2 hours in the presence or absence of heparinase (5 U/ml; Sigma-Aldrich) at 37°C. This enriched the progenitor cells and, in the presence of heparinase, allowed for cleavage of cell surface HSPGs removing ApoE, as previously described (24). Cells were then harvested and cultured for 12 hours in the specific conditions with EdU (10 μM). Heparinase-treated cells were cultured with β-DX to prevent the resynthesis for HSPGs over the course of the experiment. After incubation, cells were harvested and split into 2 samples to measure (a) cell surface ApoE and (b) proliferation (via flow cytometry).

Splenic leukocytes and HSPCs

Isolation of leukocytes or HSPCs from the spleen for flow cytometry analysis was achieved as follows. Spleens were dissected from mice perfused with PBS, and a cell suspension was obtained by manual disruption through a 40-μm cell strainer with PBS. The cellular mix was then centrifuged and subjected to a brief rbc lysis. Specific cell subsets were identified by flow cytometry as described above.

In vivo proliferation (EdU)

Mice were injected with EdU 18 hours prior to being sacrificed. Cell populations were immunostained as described above in preparation for flow cytometry. Cells were then fixed and permeabilized using 0.01% saponin

(w/v; Fluka) and 1% FCS (v/v) in IC fixation buffer (eBiosciences) for 30 minutes. Cells were then washed and stained with Alexa Fluor–conjugated azides using the Click-iT system (Invitrogen). Proliferation was quantified as percentage of EdU^+ cells by flow cytometry.

Competitive BM transplantation study

WT or *Ldlr*$^{-/-}$ mice received BM transplantation with equal portions of 8-week-old mouse BM from WT CD45.1 and WT CD45.2 *or* WT CD45.1 and *Apoe*$^{-/-}$ CD45.2. After a 6-week reconstitution period, during which mice consumed a chow diet, blood leukocyte analysis was performed. The mice were then switched to a WTD for a period of 10 weeks, during which blood leukocytes were analyzed at weeks 2, 6, and 10. At 10 weeks, the mice were sacrificed, and spleen and BM leukocytes and HSPCs were analyzed for the contribution of each respective genotype via flow cytometry. Data were calculated as a CD45.2/CD45.1 ratio.

Immunohistochemistry

Detection of CD45.1 and CD45.2 BM-derived cells in the atherosclerotic lesion in the proximal aortic root was performed on serial frozen sections as previously described (63). Briefly, sections were fixed in paraformaldehyde followed by blocking of Fc receptors (FcBlock; BD Biosciences — Pharmingen). Endogenous biotin was blocked (Vector Laboratories), and then sections were incubated with either CD45.1-biotin or CD45.2-biotin (eBiosciences). Signal amplification was achieved using a Tyramide Signal Amplification kit (Invitrogen) prior to detection with Alexa Fluor 488–conjugated streptavidin (Invitrogen). Nuclei were stained with TO-PRO-3 (Invitrogen), and transmitted light images were also captured. Lesions were viewed on a Nikon A1R multiphoton confocal microscope, and analysis was performed using NIH ImageJ. Genotype-specific BM-derived cell accumulation was quantified as CD45.1- or CD45.2-stained cells within the lesions colocalizing with nuclei.

Monocyte adhesion assay

Ly6-C^{hi} and Ly6-C^{lo} monocytes were isolated from blood by FACS, to prevent activation associated by density centrifugation (64), and then labeled with cell tracker green CMFDA (Invitrogen). Monocytes were allowed to adhere to a confluent layer of human aortic endothelial cells for 30 minutes at 37°C. Adherent monocytes were then fixed with 4% paraformaldehyde, and nonadherent cells were removed by washing with PBS. Slides were then mounted with fluorescent mounting media (Dako) and viewed on a Nikon A1R multiphoton confocal microscope. Analysis was performed using ImageJ, and the number of adherent monocytes per field was quantified.

Monocyte migration assay

Blood Ly6-C^{hi} ($CCR2^{hi}$) monocytes were isolated by FACS, seeded into the upper well of a transwell (3 μM pore; Costar), and allowed to migrate MCP-1 (CCL2) in the lower chamber for 2 hours at 37°C. The cells were then fixed with 4% paraformaldehyde, and cells that had not migrated were removed from the upper surface of the filter by scraping using cotton swabs. The filters were then stained with 1 μl/ml Hoechst (Sigma-Aldrich), mounted onto coverslip dishes, and observed via confocal microscopy (Axioskop 2 FS MOT upright confocal microscope; Zeiss). The number of cells that had migrated across the filters was determined by counting the number of cells in at least 10 random fields of images acquired with a ×10 objective at the bottom of each filter.

Lipid rafts (CTx-B)

HSPCs were isolated via FACS and plated into chamber slides (BD Falcon) precoated with poly-L-lysine (Sigma-Aldrich). Cells were allowed to adhere for 1 hour on ice, and CTx-B (Invitrogen) staining was preformed as previously described (17, 38). CTx-B staining was viewed on a Nikon A1R multiphoton confocal microscope. Analysis was performed using ImageJ.

Statistics

Statistical significance was determined by 2-tailed parametric Student's *t* test or by 1-way ANOVA (4-group comparisons) with a Bonferroni multiple-comparison post-test (GraphPad Prism). A P value less than 0.05 was considered significant. Data are mean ± SEM unless otherwise indicated.

Study approval

All patients gave their informed written consent for the study, which was approved by the Medical Ethical Committee of the Academic Medical Centre and the Dutch National Central Committee for Research Involving Humans (CCMO) and conducted in accordance with the principles of the Declaration of Helsinki. All mouse protocols were approved by the Institutional Animal Care and Use Committee of Columbia University.

Acknowledgments

This work was supported by NIH grants HL107653 and 54591 and by the Foundation Leducq. M. Akhtari was a research fellow supported by the Sarnoff Cardiovascular Research Foundation. M. Sanson is supported by NIH grant HL-084312. L. Yvan-Charvet is a recipient of American Heart Association grant SDG2160053. The authors thank the flow cytometry unit at Columbia University for HSPC sorting, George Kuriakose for atherosclerotic lesion sectioning, and CSL Australia for providing the rHDL used in this study.

Received for publication May 20, 2011, and accepted in revised form August 10, 2011.

Address correspondence to: Andrew J. Murphy, Division of Molecular Medicine, 630 W 168th St., Room 8-401, Columbia University, New York, New York 10032, USA. Phone: 212.305.5789; Fax: 212.305.5052; E-mail: am3440@columbia.edu.

1. Coller BS. Leukocytosis and ischemic vascular disease morbidity and mortality: is it time to intervene? *Arterioscler Thromb Vasc Biol*. 2005;25(4):658–670.
2. Lee YJ, Shin YH, Kim JK, Shim JY, Kang DR, Lee HR. Metabolic syndrome and its association with white blood cell count in children and adolescents in Korea: The 2005 Korean National Health and Nutrition Examination Survey. *Nutr Metab Cardiovasc Dis*. 2010;20(3):165–172.
3. Ortlepp JR, Metrikat J, Albrecht M, Maya-Pelzer P. Relationship between physical fitness and lifestyle behaviour in healthy young men. *Eur J Cardiovasc Prev Rehabil*. 2004;11(3):192–200.
4. Bovill EG, et al. White blood cell counts in persons aged 65 years or more from the Cardiovascular Health Study. Correlations with baseline clinical and demographic characteristics. *Am J Epidemiol*. 1996;143(11):1107–1115.
5. Tani S, et al. Association of leukocyte subtype counts with coronary atherosclerotic regression following pravastatin treatment. *Am J Cardiol*. 2009; 104(4):464–469.
6. Chapman CM, Beilby JP, McQuillan BM, Thompson PL, Hung J. Monocyte count, but not C-reactive protein or interleukin-6, is an independent risk marker for subclinical carotid atherosclerosis. *Stroke*. 2004;35(7):1619–1624.
7. Afiune Neto A, Mansur Ade P, Avakian SD, Gomes EP, Ramires JA. [Monocytosis is an independent risk marker for coronary artery disease]. *Arq Bras Cardiol*. 2006;86(3):240–244.
8. Stewart RA, et al. White blood cell count predicts reduction in coronary heart disease mortality with pravastatin. *Circulation*. 2005;111(14):1756–1762.
9. Feldman DL, Mogelesky TC, Liptak BF, Gerrity RG. Leukocytosis in rabbits with diet-induced atherosclerosis. *Arterioscler Thromb*. 1991;11(4):985–994.
10. Averill LE, Meagher RC, Gerrity RG. Enhanced monocyte progenitor cell proliferation in bone marrow of hyperlipemic swine. *Am J Pathol*. 1989; 135(2):369–377.
11. Swirski FK, et al. Ly-6Chi monocytes dominate hypercholesterolemia-associated monocytosis and give rise to macrophages in atheromata. *J Clin Invest*. 2007;117(1):195–205.
12. Tacke F, et al. Monocyte subsets differentially employ CCR2, CCR5, and CX3CR1 to accumulate within atherosclerotic plaques. *J Clin Invest*.

2007;117(1):185–194.
13. Drechsler M, Megens RT, van Zandvoort M, Weber C, Soehnlein O. Hyperlipidemia-triggered neutrophilia promotes early atherosclerosis. *Circulation*. 2010;122(18):1837–1845.
14. Zernecke A, et al. Protective role of CXC receptor 4/CXC ligand 12 unveils the importance of neutrophils in atherosclerosis. *Circ Res*. 2008;102(2):209–217.
15. Yvan-Charvet L, Wang N, Tall AR. Role of HDL, ABCA1, and ABCG1 transporters in cholesterol efflux and immune responses. *Arterioscler Thromb Vasc Biol*. 2010;30(2):139–143.
16. Yvan-Charvet L, et al. Combined deficiency of ABCA1 and ABCG1 promotes foam cell accumulation and accelerates atherosclerosis in mice. *J Clin Invest*. 2007;117(12):3900–3908.
17. Yvan-Charvet L, et al. ATP-binding cassette transporters and HDL suppress hematopoietic stem cell proliferation. *Science*. 2010;328(5986):1689–1693.
18. Matsuura F, Wang N, Chen W, Jiang XC, Tall AR. HDL from CETP-deficient subjects shows enhanced ability to promote cholesterol efflux from macrophages in an apoE- and ABCG1-dependent pathway. *J Clin Invest*. 2006;116(5):1435–1442.
19. Remaley AT, et al. Apolipoprotein specificity for lipid efflux by the human ABCAI transporter. *Biochem Biophys Res Commun*. 2001;280(3):818–823.
20. Goodrum JF, Bouldin TW, Zhang SH, Maeda N, Popko B. Nerve regeneration and cholesterol reutilization occur in the absence of apolipoproteins E and A-I in mice. *J Neurochem*. 1995;64(1):408–416.
21. Weissman IL, Shizuru JA. The origins of the identification and isolation of hematopoietic stem cells, and their capability to induce donor-specific transplantation tolerance and treat autoimmune diseases. *Blood*. 2008;112(9):3543–3553.
22. Wilson A, et al. Hematopoietic stem cells reversibly switch from dormancy to self-renewal during homeostasis and repair. *Cell*. 2008;135(6):1118–1129.
23. Forsberg EC, Prohaska SS, Katzman S, Heffner GC, Stuart JM, Weissman IL. Differential expression of novel potential regulators in hematopoietic stem cells. *PLoS Genet*. 2005;1(3):e28.
24. Lucas M, Mazzone T. Cell surface proteoglycans modulate net synthesis and secretion of macrophage apolipoprotein E. *J Biol Chem*. 1996; 271(23):13454–13460.
25. Fazio S, Babaev VR, Burleigh ME, Major AS, Hasty AH, Linton MF. Physiological expression of macrophage apoE in the artery wall reduces atherosclerosis in severely hyperlipidemic mice. *J Lipid Res*. 2002;43(10):1602–1609.
26. Fazio S, et al. Increased atherosclerosis in mice reconstituted with apolipoprotein E null macrophages. *Proc Natl Acad Sci U S A*. 1997;94(9):4647–4652.
27. Potteaux S, et al. Suppressed monocyte recruitment drives macrophage removal from atherosclerotic plaques of Apoe$^{-/-}$ mice during disease regression. *J Clin Invest*. 2011;121(5):2025–2036.
28. Dietrich C, Volovyk ZN, Levi M, Thompson NL, Jacobson K. Partitioning of Thy-1, GM1, and cross-linked phospholipid analogs into lipid rafts reconstituted in supported model membrane monolayers. *Proc Natl Acad Sci U S A*. 2001;98(19):10642–10647.
29. Fessler MB, et al. Lipid rafts regulate lipopolysaccharide-induced activation of Cdc42 and inflammatory functions of the human neutrophil. *J Biol Chem*. 2004;279(38):39989–39998.
30. Nichols BJ. GM1-containing lipid rafts are depleted within clathrin-coated pits. *Curr Biol*. 2003; 13(8):686–690.
31. Han X, Kitamoto S, Wang H, Boisvert WA. Interleukin-10 overexpression in macrophages suppresses atherosclerosis in hyperlipidemic mice. *FASEB J*. 2010;24(8):2869–2880.
32. Igarashi M, et al. Targeting of neutral cholesterol ester hydrolase to the endoplasmic reticulum via its N-terminal sequence. *J Lipid Res*. 2010;51(2):274–285.
33. Lunghi P, et al. Downmodulation of ERK activity inhibits the proliferation and induces the apoptosis of primary acute myelogenous leukemia blasts. *Leukemia*. 2003;17(9):1783–1793.
34. Moriggl R, et al. Stat5 tetramer formation is associated with leukemogenesis. *Cancer Cell*. 2005; 7(1):87–99.
35. Mui AL, Wakao H, O'Farrell AM, Harada N, Miyajima A. Interleukin-3, granulocyte-macrophage colony stimulating factor and interleukin-5 transduce signals through two STAT5 homologs. *EMBO J*. 1995;14(6):1166–1175.
36. Nosaka T, Kawashima T, Misawa K, Ikuta K, Mui AL, Kitamura T. STAT5 as a molecular regulator of proliferation, differentiation and apoptosis in hematopoietic cells. *EMBO J*. 1999;18(17):4754–4765.
37. Christian AE, Haynes MP, Phillips MC, Rothblat GH. Use of cyclodextrins for manipulating cellular cholesterol content. *J Lipid Res*. 1997;38(11):2264–2272.
38. Murphy AJ, et al. High-density lipoprotein reduces the human monocyte inflammatory response. *Arterioscler Thromb Vasc Biol*. 2008;28(11):2071–2077.
39. Tardif JC, et al. Effects of reconstituted high-density lipoprotein infusions on coronary atherosclerosis: a randomized controlled trial. *JAMA*. 2007; 297(15):1675–1682.
40. Swirski FK, et al. Identification of splenic reservoir monocytes and their deployment to inflammatory sites. *Science*. 2009;325(5940):612–616.
41. O'Malley DP, Kim YS, Perkins SL, Baldridge L, Juliar BE, Orazi A. Morphologic and immunohistochemical evaluation of splenic hematopoietic proliferations in neoplastic and benign disorders. *Mod Pathol*. 2005;18(12):1550–1561.
42. Wilkins BS, Green A, Wild AE, Jones DB. Extramedullary haemopoiesis in fetal and adult human spleen: a quantitative immunohistological study. *Histopathology*. 1994;24(3):241–247.
43. Lin CY, Duan H, Mazzone T. Apolipoprotein E-dependent cholesterol efflux from macrophages: kinetic study and divergent mechanisms for endogenous versus exogenous apolipoprotein E. *J Lipid Res*. 1999;40(9):1618–1627.
44. Qiao JH, et al. Role of macrophage colony-stimulating factor in atherosclerosis: studies of osteopetrotic mice. *Am J Pathol*. 1997;150(5):1687–1699.
45. Rajavashisth T, et al. Heterozygous osteopetrotic (op) mutation reduces atherosclerosis in LDL receptor-deficient mice. *J Clin Invest*. 1998;101(12):2702–2710.
46. Smith JD, Trogan E, Ginsberg M, Grigaux C, Tian J, Miyata M. Decreased atherosclerosis in mice deficient in both macrophage colony-stimulating factor (op) and apolipoprotein E. *Proc Natl Acad Sci U S A*. 1995;92(18):8264–8268.
47. Stoneman V, et al. Monocyte/macrophage suppression in CD11b diphtheria toxin receptor transgenic mice differentially affects atherogenesis and established plaques. *Circ Res*. 2007;100(6):884–893.
48. Linton MF, Atkinson JB, Fazio S. Prevention of atherosclerosis in apolipoprotein E-deficient mice by bone marrow transplantation. *Science*. 1995; 267(5200):1034–1037.
49. Innerarity TL, Arnold KS, Weisgraber KH, Mahley RW. Apolipoprotein E is the determinant that mediates the receptor uptake of beta-very low density lipoproteins by mouse macrophages. *Arteriosclerosis*. 1986;6(1):114–122.
50. Bellosta S, et al. Macrophage-specific expression of human apolipoprotein E reduces atherosclerosis in hypercholesterolemic apolipoprotein E-null mice. *J Clin Invest*. 1995;96(5):2170–2179.
51. Rong JX, et al. Elevating high-density lipoprotein cholesterol in apolipoprotein E-deficient mice remodels advanced atherosclerotic lesions by decreasing macrophage and increasing smooth muscle cell content. *Circulation*. 2001;104(20):2447–2452.
52. Murphy AJ, et al. Neutrophil activation is attenuated by high-density lipoprotein and apolipoprotein a-I in in vitro and in vivo models of inflammation. *Arterioscler Thromb Vasc Biol*. 2011;31(6):1333–1341.
53. Patel S, et al. Reconstituted high-density lipoprotein increases plasma high-density lipoprotein anti-inflammatory properties and cholesterol efflux capacity in patients with type 2 diabetes. *J Am Coll Cardiol*. 2009;53(11):962–971.
54. Shaw JA, et al. Infusion of reconstituted high-density lipoprotein leads to acute changes in human atherosclerotic plaque. *Circ Res*. 2008;103(10):1084–1091.
55. Blaschke F, et al. A nuclear receptor corepressor-dependent pathway mediates suppression of cytokine-induced C-reactive protein gene expression by liver X receptor. *Circ Res*. 2006;99(12):e88–e99.
56. Funke H, et al. A molecular defect causing fish eye disease: an amino acid exchange in lecithin-cholesterol acyltransferase (LCAT) leads to the selective loss of alpha-LCAT activity. *Proc Natl Acad Sci U S A*. 1991;88(11):4855–4859.
57. Holleboom AG, et al. High prevalence of mutations in LCAT in patients with low high-density lipoprotein cholesterol levels in The Netherlands: Identification and characterization of 8 new mutations in LCAT [published online ahead of print September 7, 2011]. *Hum Mutat*. doi:10.1002/humu.21578.
58. Idzior-Walus B, et al. Familial lecithin-cholesterol acyltransferase deficiency: biochemical characteristics and molecular analysis of a new LCAT mutation in a Polish family. *Atherosclerosis*. 2006; 185(2):413–420.
59. Candini C, et al. Identification and characterization of novel loss of function mutations in ATP-binding cassette transporter A1 in patients with low plasma high-density lipoprotein cholesterol. *Atherosclerosis*. 2010;213(2):492–498.
60. Hovingh GK, et al. HDL deficiency and atherosclerosis: lessons from Tangier disease. *J Intern Med*. 2004;255(2):299–301.
61. Yvan-Charvet L, et al. Increased inflammatory gene expression in ABC transporter-deficient macrophages: free cholesterol accumulation, increased signaling via toll-like receptors, and neutrophil infiltration of atherosclerotic lesions. *Circulation*. 2008;118(18):1837–1847.
62. Gower RM, et al. CD11c/CD18 expression is upregulated on blood monocytes during hypertriglyceridemia and enhances adhesion to vascular cell adhesion molecule-1. *Arterioscler Thromb Vasc Biol*. 2011;31(1):160–166.
63. Llodrá J, Angeli V, Liu J, Trogan E, Fisher EA, Randolph GJ. Emigration of monocyte-derived cells from atherosclerotic lesions characterizes regressive, but not progressive, plaques. *Proc Natl Acad Sci U S A*. 2004;101(32):11779–11784.
64. Cros J, et al. Human CD14dim monocytes patrol and sense nucleic acids and viruses via TLR7 and TLR8 receptors. *Immunity*. 2010;33(3):375–386.